Transition Between Coherent and Incoherent Electron Transport in GaAs/GaAlAs Superlattices

C. Rauch, G. Strasser, K. Unterrainer, W. Boxleitner, and E. Gornik
Institute for Solid State Electronics and Center for Microstructures, University of Technology Vienna, A-1040 Wien, Austria

A. Wacker
Institute for Theoretical Physics, Technical University Berlin, D-10623 Berlin, Germany
(Received 21 November 1997)

The transition between coherent and incoherent transport in undoped GaAs/AlGaAs superlattices is observed. Hot electron spectroscopy is used to measure the superlattice transmittance at different bias conditions. For a short-period superlattice the transmittance is found to be independent of the direction of the electric field. For a superlattice larger than the coherence length, the transmission becomes asymmetric and dependent on the electric field direction. The onset of scattering-induced miniband transport is clearly evident. A coherence length of 150 nm, limited by surface roughness, and a scattering time of 1 ps are determined. [S0031-9007(98)07370-0]

PACS numbers: 73.20.Dx, 72.80.Ey, 73.40.Gk

In semiconductor superlattices (SL) the energy levels of adjacent wells are strongly coupled, and their wave functions are delocalized which leads to the formation of minibands. Electron transport in superlattice minibands was first considered by Esaki and Tsu [1], who reported that a region of negative differential conductivity should occur when the electrons are accelerated to the miniband zone boundary. In a finite electric field, applied to a periodic structure, the quantum mechanical eigenstates are given by the Wannier-Stark states [2] which are localized to a region whose extension is inversely proportional to the electric field. If the length of the superlattice is shorter than this extension coherent transmission through an ideal SL is possible [3]. In contrast, for infinite superlattices the pure coherent transmission through the SL is zero, and Bloch oscillations are expected (see, e.g., Refs. [3,4]). In this case, only the presence of scattering causes the decay of the Bloch oscillations and induces a finite stationary current through the SL [5,6]. The transition between coherent transmission through a small structure and diffusive transport in a long SL is not well understood. It is the purpose of our Letter to demonstrate this transition experimentally and to explain the underlying scattering mechanism.

Resonant tunneling phenomena have been extensively studied in double barrier structures [7] where the current is calculated by the single particle Schrödinger equation assuming that the electrons move coherently, while loss of coherence requires more sophisticated models [8]. Transport in superlattices has been studied extensively in the last two decades [9–13]. Photocurrent spectroscopy has been used to measure the quantum coherence in GaAs/GaAlAs superlattices optically [14,15]. The study of biased superlattices, however, was hindered by space charge built up and domain formation [16]. Sibille *et al.* [17,18] performed the most extensive study in biased, doped superlattices and observed negative differential velocity. Optical experiments led to a breakthrough by the observation of Bloch oscillations in the time domain of undoped superlattices [19].

In a previous experiment we have developed a three terminal technique which allowed the study of transport in undoped superlattices [20]. We observed the positions of minibands and minigaps in excellent agreement with the results of a transfer-matrix calculation of the tunneling probability. In the present paper we apply the technique of hot electron spectroscopy to biased superlattices. We observe the transition between coherent and incoherent transport and determine the coherence length and the scattering time of the electrons.

A three terminal device [21] is used to probe the transmittance of undoped $GaAs/Ga_{0.7}Al_{0.3}As$ superlattices. An energy tunable electron beam is generated by a tunneling barrier and passes the superlattice after traversing a thin highly doped n-GaAs base layer and an undoped drift region. The measured collector current reflects the probability of an injected electron to be transmitted through the superlattice. The transmittance of the superlattice can be measured directly at given superlattice bias conditions by varying the energy of the injected hot electrons independently from the superlattice bias voltage.

The structures which are described in Fig. 1 were grown by molecular beam epitaxy on semi-insulating GaAs substrate. The growth started with a highly doped n^+-GaAs collector contact layer ($n = 1 \times 10^{18}$ cm^{-3}) followed by a superlattice and the drift region that is slightly n doped ($n \sim 5 \times 10^{14}$ cm^{-3}) in order to avoid undesired band bending. To reduce quantum mechanical confining effects originating from the quantum well formed by the emitter barrier and the superlattice, the drift region is chosen to be 200 nm width. This is followed by a highly doped ($n = 2 \times 10^{18}$ cm^{-3}) n^+-GaAs

layer (base) of 13 nm width. As found in previous experiments, about 60% of the injected electrons traverse the base ballistically. On top of the base layer a 13 nm undoped $Ga_{0.7}Al_{0.3}As$ barrier is grown followed by a GaAs space and an n^+-GaAs layer, nominally doped to $n = 3 \times 10^{17}$ cm^{-3}, in order to achieve a narrow normal energy distribution of the injected electrons of about 17 meV [22]. The width of the injected electron beam limits the energy resolution of the experiment. Finally, an n^+-GaAs contact layer ($n = 1 \times 10^{18}$ cm^{-3}) is grown on top of the heterostructure to form the emitter.

Selective etching of 20×20 μm^2 mesas was used to reach the base layer. The Ohmic contacts are formed using a standard AuGe/Ni alloy. Details can be found in Ref. [20].

A series of superlattice structures was investigated consisting of 5, 10, 20, and 30 periods of 2.5 nm $Ga_{0.7}Al_{0.3}As$ barriers and 6.5 nm GaAs wells. The layer structure was verified by transmission electron microscopy (TEM). For these parameters a simple Kronig-Penny calculation gives the lowest miniband lying between 46 and 68 meV, and a second one between 182 and 276 meV. We have found a systematic change of the transport properties between the 5 and 30 period samples resembling the transition between coherent to incoherent transport.

The static transfer ratio $\alpha = I_C/I_E$ [23] is measured as a function of negative emitter bias (= injected electron energy) at 4.2 K in a common base configuration. Typical static transfer ratios α of the 20 period superlattice is shown in Fig. 2 for different collector biases. No collector current is observed up to the first transparent state of the first miniband, indicating that there is no significant leakage current between base and collector. The black solid line represents the transfer ratio at flat band condition ($U_{BC} = 0$). The sharp increase of the transfer ratio at about 45 meV coincides very well with the lower edge of the first miniband which is calculated to be 46 meV. The peak due to transport through the first maniband is broader than the expected miniband width ($\Delta = 22$ meV) due to the finite width of the injected electron distribution. The second observed peak is shifted 36 meV to higher injection energies and is ascribed to the first longitudinal optical (LO)-phonon emission replica ($\hbar\omega_{LO} = 36$ meV). Assuming an optical phonon scattering time of 200 fs at 100 meV electron energy and an electron velocity of 7.2×10^5 m/s, about 80% of the injected electrons are scattered in the drift region and lose 36 meV in energy. This results in a nonvanishing transfer ratio between the peaks since the full width at half maximum (FWHM) of the injected electron distribution (17 meV) plus the width of the first miniband (22 meV) is greater than the LO-phonon energy. Superposition of the replicas and the nonscattered electrons leads to the observed behavior in the transfer ratio as evident in the experiment (Fig. 2). Even the second LO-phonon replica, shifted by 72 meV to higher energies is observed. The sharp increase of the transmittance at about 180 meV is due to transport through the second superlattice miniband. A clear shift of the maximum (due to the voltage drop in the drift region) and a reduction of the amplitude of the transfer ratio is observed for negative collector voltages. After a first increase a significant lower reduction of the amplitude and of the shift is observed for increasing positive collector biases. A plot of the tunnel current onsets versus injection energy is shown in the inset of Fig. 2. The extrapolation of the different slopes to the cross point identifies the flat band condition with high accuracy.

We have taken the total miniband transmission (T_α) which is defined as twice the area of the lower energy side of the first transfer ratio peak as a measure for the average current through the first miniband at given bias conditions.

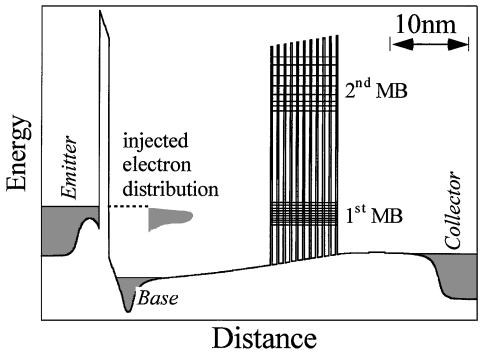

FIG. 1. Schematic band diagram of a three terminal device with negative bias applied to the superlattice.

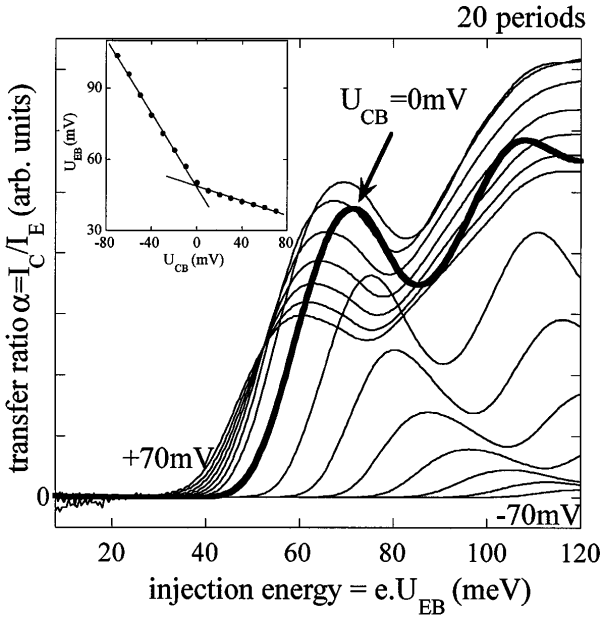

FIG. 2. Transfer ratio α versus injection energy at different collector base voltages (U_{CB}) of the 20 period sample for U_{CB} steps of 20 mV. The solid black line represents the transfer ratio under flat band condition ($U_{CB} = 0$). The inset shows the emitter voltage (U_{EB}) of the onsets of the transfer ratio at different collector-base (U_{CB}) voltages.

The current above the first maximum is influenced by the first LO-phonon replica and, thus, not used for the determination of T_α. The analysis of T_α for the 5, 10, 20, and 30 period superlattices is shown in Fig. 3 over the voltage applied across the superlattice. The electric field is inversely proportional to the superlattice period number. The total miniband transmission T_α (dots) of the 5 period sample is symmetric for both bias directions, while clear asymmetric behavior is observed for all the other samples, where the asymmetry is growing with the period number. The experimental T_α curves are shifted for clarity, but cannot be compared directly in absolute terms since the current values for different samples of the same period vary by $\pm 30\%$.

In order to understand our findings we have performed two different kinds of calculations for the transmission through the superlattice. In the first calculation we consider a one dimensional ideal structure with normal sample parameters. The calculation of the transmission is based on a transfer matrix method using an envelope function approximation, which also includes nonparabolicity. The result of this calculation demonstrates the quenching of the current as a function of the applied electric field [24]. This can be easily understood by the increasing localization of the Wannier-Stark states. By summing up the contributions to the current for all injection energies we obtain the transmission T_α as shown by a dashed line in Fig. 3. Independently of the length of the superlattice, this curve is symmetric with respect to the field direction as the quenching of the Wannier-Stark states depends only on the absolute value of the electric field. This calculation agrees quite well with the experiment for the 5 period superlattice (dots), demonstrating that the transport is dominated by coherent transmission in this case.

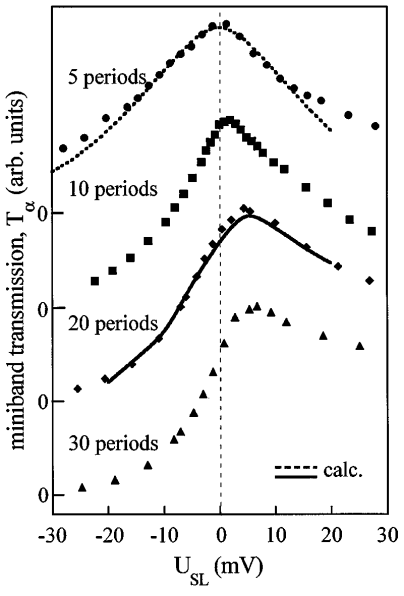

FIG. 3. Miniband transmission versus electric field of the 5, 10, 20, and 30 period samples. The miniband transmission of the 5 period sample (dots) is compared to a one dimensional calculation (dashed line) for coherent transmission while the results of the 20 period sample (diamonds) are compared to a calculation including interface roughness (solid line).

However, the picture changes for samples with more periods (Fig. 3): For negative bias (decelerating field) the measured current decays systematically faster with superlattice bias and shows reduced current with increased period number. For positive bias the current first increases and the maximum extends to higher voltages the larger the period number.

We assign the observed systematic behavior with increasing superlattice period to the onset of diffusive transport. For a longer superlattice (starting with period 10) only a small fraction of the carriers can traverse the structure without scattering. Typically, the scattering process decreases the kinetic electron energy in the transport direction, either by transferring the energy difference to a motion perpendicular to the SL direction (elastic scattering) or by exciting a phonon (inelastic). If a positive bias is applied to the collector, we observe an increase of the transfer ratio since the scattered electrons contribute additionally with the coherent electrons to the collector current. For the negative bias only coherent electrons traverse the superlattice, scattered electrons are flowing back to the base according to the applied electric field. Therefore the presence of scattering destroys the symmetry of the transmission with respect to the field direction.

In order to check this reasoning we have performed a second calculation for the transmission through a full three dimensional structure where interface roughness is included. We use a typical island size of 10 nm, and the calculation is performed analogously to Ref. [25]. As shown in Fig. 3 (solid line), the calculated transmission for the 20 period sample becomes asymmetric in excellent agreement with the experimental result (diamonds). This clearly demonstrates that scattering by interface roughness induces the asymmetry.

From these findings we conclude that the transition from coherent transmission to diffusive transport occurs visibly between 5 and 10 periods for the structures used. The main scattering mechanism is interface roughness in these undoped structures at a temperature of 4.2 K. Phonon scattering seems to be negligible as the transmissions does not change with temperature up to 40 K.

Following our reasoning given above, the transmission for negative fields is mainly due to the fraction of electrons traversing the structure without scattering. This ballistic part (dashed line) is symmetric with respect to the field and can be subtracted from the total transmission for positive electric fields as shown in Fig. 4 for the 20 period sample. The difference (open squares) can then be interpreted as the scattering induced current, which is found to be in excellent agreement with the Esaki-Tsu model [1] using a scattering time τ_{scatt} of 1 ps. The average velocity in the miniband is of the order

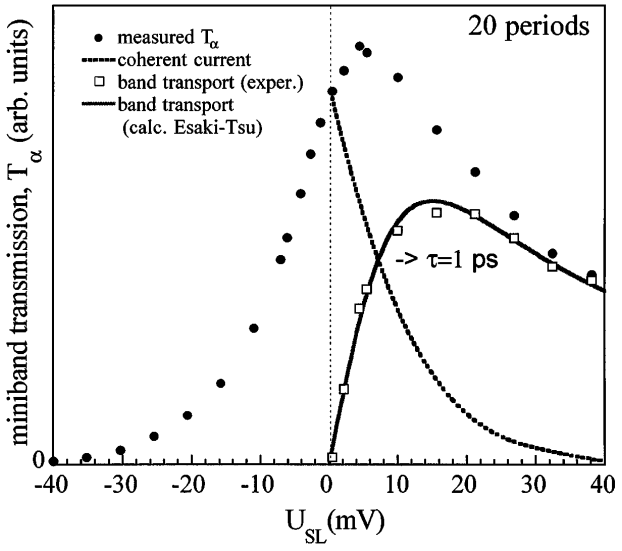

FIG. 4. Total miniband transmission versus electric field of the 20 period superlattice (dots). For positive applied bias, the coherent part (dashed line) is subtracted from the data to give the incoherent current (squares). The incoherent current is fitted using the Esaki-Tsu formula (solid line).

of $\Delta d/2\hbar = 1.5 \times 10^7$ cm/s where d is the superlattice period and Δ the miniband width. This results in a mean free path of $\ell_{\mathrm{coh}} = \nu\tau_{\mathrm{scatt}} = 150$ nm. This length is significantly larger than the 5 period superlattice (45 nm) in good agreement with our interpretation that ballistic transport dominates the short structure, while scattering becomes important for the longer superlattices.

The scattering time of $\tau = 1$ ps appears quite reasonable for transport in an undoped superlattice. The coherent transmission time is estimated for the individual Stark state to be 0.6 ps for the 5 period superlattice which increases to 1.2 ps for the 10 period superlattice. This times are consistent with the onset of scattering at the 10 period superlattice. The coherence length of 150 nm thus is longer in our undoped superlattice structures than the length reported from cyclotron resonance measurements for doped superlattices [26].

In summary, we have observed the transition between resonant tunneling and band transport in a solid using vertical tunneling through biased semiconductor superlattices. The band transport is induced by scattering and overcomes the localization of the electron wave functions introduced by an applied electric field. Furthermore we have determined the scattering time and the coherence length (150 nm) of the electrons in these superlattices. We have shown that the coherent transport in the investigated superlattices at 4.2 K is limited by interface roughness. The present results provide the basis for further systematic studies of superlattice transport by varying growth conditions, local doping, and band structure.

This work has been partly supported by the Austrian Federal Ministry of Science, the Society for Microelectronics (GMe, Austria), the Fond zur Förderung der Wissenschaft und Forschung, and the U.S. Army Research Office. Helpful discussions with S. Bose and B. Y.-K. Hu are acknowledged.

[1] L. Esaki and R. Tsu, IBM J. Res. Dev. **14**, 61 (1970).
[2] G. H. Wannier, Phys. Rev. **117**, 432 (1960).
[3] R. Tsu and L. Esaki, Appl. Phys. Lett. **22**, 562 (1973).
[4] J. B. Krieger and G. J. Iafrate, Phys. Rev. B **33**, 5494 (1986).
[5] R. A. Suris and B. S. Shchamkhalova, Sov. Phys. Semicond. **18**, 738 (1984).
[6] R. Tsu and G. Döhler, Phys. Rev. B **12**, 680 (1975).
[7] P. H. Beton, J. Wang, N. Mori, L. Eaves, P. C. Main, T. J. Foster, and M. Henini, Phys. Rev. Lett. **75**, 1996 (1995).
[8] W. R. Frensley, Rev. Mod. Phys. **62**, 745 (1990).
[9] L. Esaki and L. L. Chang, Phys. Rev. Lett. **33**, 495 (1974).
[10] F. Beltram, F. Capasso, D. L. Sivco, A. L. Hutchinson, S-N. G. Chu, and A. Y. Cho, Phys. Rev. Lett. **64**, 3167 (1990).
[11] P. Voisin, J. Bleuse, C. Bouche, S. Gaillard, C. Alibert, and A. Regreny, Phys. Rev. Lett. **61**, 1639 (1988); J. Bleuse, P. Voisin, M. Allovon, and M. Quillec, Appl. Phys. Lett. **53**, 2632 (1988).
[12] P. England, M. Helm, J. R. Hayes, J. P. Harbison, E. Colas, and L. T. Florez, Appl. Phys. Lett. **54**, 647 (1989).
[13] G. Brozak, M. Helm, F. DeRosa, C. H. Perry, M. Koza, R. Bhat, and S. J. Allen, Phys. Rev. Lett. **64**, 3163 (1990).
[14] E. E. Mendez, F. Agulló-Rueda, and J. M. Hong, Phys. Rev. Lett. **60**, 2426 (1988).
[15] F. Agulló-Rueda, E. E. Mendez, and J. M. Hong, Phys. Rev. B **40**, 1357 (1989).
[16] H. T. Grahn, R. J. Haug, W. Müller, and K. Ploog, Phys. Rev. Lett. **67**, 1618 (1991).
[17] A. Sibille, J. F. Palmier, H. Wang, and F. Mollot, Phys. Rev. Lett. **64**, 52 (1990).
[18] A. Sibille, J. F. Palmier, and F. Mollot, Appl. Phys. Lett. **60**, 52 (1992).
[19] Ch. Waschke, H. G. Roskos, R. Schwedler, K. Leo, H. Kurz, and K. Köhler, Phys. Rev. Lett. **70**, 3319 (1993).
[20] C. Rauch, G. Strasser, K. Unterrainer, B. Brill, and E. Gornik, Appl. Phys. Lett. **70**, 649 (1997).
[21] M. Heiblum, M. I. Nathan, D. C. Thomas, and C. M. Knoedler, Phys. Rev. Lett. **55**, 2200 (1985).
[22] G. Strasser, C. Rauch, and E. Gornik (to be published).
[23] The transfer ratio $\alpha = I_C/I_E$, where I_E is the injected current and I_C is the collected current, measures the probability for electrons to be collected after traversing the superlattice at given injection energies.
[24] C. Rauch, G. Strasser, K. Unterrainer, W. Boxleitner, and E. Gornik, Phys. Status Solidi (b) **204**, 393 (1997).
[25] D. Z.-Y. Ting and T. C. McGill, in *Quantum Transport in Ultrasmall Devices*, edited by D. K. Ferry *et al.* (Plenum, New York, 1995), pp. 417–436.
[26] T. Duffield, R. Bhat, M. Koza, F. DeRosa, D. M. Hwang, P. Grabbe, and S. J. Allen, Phys. Rev. Lett. **56**, 2724 (1986).